Fluorescence resonance energy transfer and molecular modeling studies on 4′,6-diamidino-2-phenylindole (DAPI) complexes with tubulin

JOSÉ J. ARBILDUA,[1] JUAN E. BRUNET,[2] DAVID M. JAMESON,[3] MARIBEL LÓPEZ,[1] ESTEBAN NOVA,[1] ROSALBA LAGOS,[1] AND OCTAVIO MONASTERIO[1]

[1]Departamento de Biología, Facultad de Ciencias, Universidad de Chile, Casilla 653, Santiago, Chile
[2]Instituto de Química, Facultad de Ciencias Básicas y Matemáticas, Pontificia Universidad Católica de Valparaíso, Casilla 4059, Valparaiso, Chile
[3]Department of Cell and Molecular Biology, John A. Burns School of Medicine, University of Hawaii, Honolulu, Hawaii

Abstract

The goal of this work was to determine the binding properties and location of 4′,6-diamidino-2-phenylindole (DAPI) complexed with tubulin. Using fluorescence anisotropy, a dissociation constant of 5.2 ± 0.4 μM for the DAPI–tubulin complex was determined, slightly lower than that for the tubulin S complex. The influence of the C-terminal region on the binding of DAPI to tubulin was also characterized. Using FRET experiments, and assuming a κ^2 value of 2/3, distances between Co^{2+} bound to its high-affinity binding site and the DAPI-binding site and 2′,3′-O-(trinitrophenyl)guanosine 5′-triphosphate bound to the exchangeable nucleotide and the DAPI-binding site were found to be 20 ± 2 Å and 43 ± 2 Å, respectively. To locate potential DAPI-binding sites on tubulin, a molecular modeling study was carried out using the tubulin crystal structure and energy minimization calculations. The results from the FRET measurements were used to limit the possible location of DAPI in the tubulin structure. Several candidate binding sites were found and these are discussed in the context of the various properties of bound DAPI.

Keywords: tubulin; DAPI; TNP–GTP; FRET; molecular docking

The major structural component of microtubules is tubulin, a heterodimer composed of α- and β-tubulin (Bryan and Wilson 1971). The structure of the heterodimer with GDP and GTP bound to the exchangeable (E-site) and to the nonexchangeable nucleotide site (N-site), respectively, and with taxol bound to β-tubulin, has been resolved by electron crystallography of zinc-induced tubulin sheets (Nogales et al. 1998a). A high-resolution model of microtubule has been obtained by docking the structure of the tubulin heterodimer into an 8-Å map of microtubule (Huilin et al. 2002). However, little is known about the location of several compounds that presumably bind to particular binding sites. This lack of information raises questions concerning the spatial distribution of these sites and their influence on tubulin contacts in the various tubulin polymers. In tubulin, intrinsic and extrinsic fluorescent probes have been used in conjunction with FRET methodologies to measure dis-

Reprint requests to: Octavio Monasterio, Departamento de Biología, Facultad de Ciencias, Universidad de Chile, Casilla 653, Santiago, Chile; e-mail: monaster@uchile.cl; fax: 56-2-276-3870.

Abbreviations: C-terminal, carboxyl terminal; DAPI, 4′,6-diamidino-2-phenylindole; EGTA, ethylene glycol bis(β-aminoethyl ether)-N,N′-tetraacetic acid; FRET, fluorescence resonance energy transfer; GTP, Guanosine 5′-triphosphate; PIPES, Piperazine-1,4-bis(2-ethanesufonic acid); MES, 2-Morpholinoethanesulfonic acid; N-terminal, amino terminal; PVA, poly(vinyl) alcohol; SDS, sodium dodecyl sulfate; TEA, triethanolamine; Tris, tris(hydroxymethyl) aminomethane; TNP-GTP, 2′,3′-*O*-(trinitrophenyl)guanosine 5′-triphosphate; tubulin S, subtilisin cleaved tubulin dimer.

tances (Ward and Timassheff 1988; Bhattacharyya et al. 1993, 1996; Ward et al. 1994; Han et al. 1998) to monitor tubulin conformational changes (Prasad et al. 1986; Bhattacharyya et al. 1994; Soto et al. 1996) and to follow tubulin polymerization (Bonne et al. 1985; Kung and Reed 1989). However, the location and nature of the fluorescent probe binding sites in general have been poorly characterized.

DAPI, a polycationic fluorescent reagent, first synthesized by Grossgebauer et al. (1976) for use as a trypanocidal drug, has been shown to bind to DNA (Russell et al. 1975; Hajduk 1976; Barcellona and Gratton 1990) and to proteins, including tubulin (Mazzini et al. 1992). Quenching of DAPI's fluorescence and a red shift of its fluorescence maximum upon binding to the tubulin heterodimer results when the C-terminal tubulin region is removed by controlled digestion with subtilisin (Ortiz et al. 1993), specifically when the last 12–15 amino acids of the negatively charged C-terminal region of both α- and β-tubulin are removed, giving tubulin S (Melki et al. 1991; Monasterio et al. 1995). The fluorescence properties are partially restored when the C-terminal peptides are added back to tubulin S (Bonne et al. 1985; Ortiz et al. 1993). Therefore, DAPI (Fig. 1) appears to be an appropriate fluorescence probe to study the role of the C-terminal region in tubulin function.

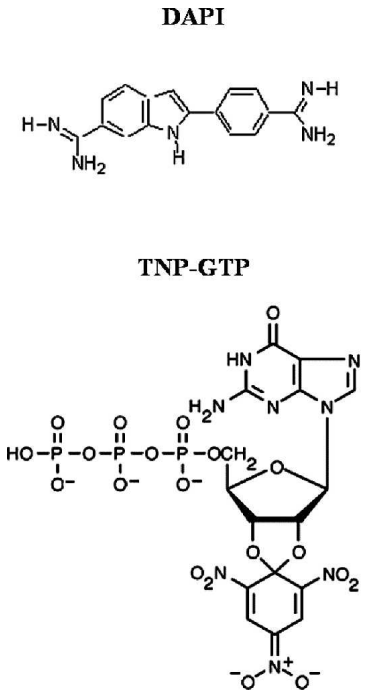

Figure 1. Structures of 4′-6-diamidino-2-phenylindole (DAPI) and 2′,3′-*O*-(2,4,6-trinitrocyclohexadienylidene)-GTP (TNP-GTP) at neutral or basic pH.

Several studies have demonstrated that the C-terminal region of tubulin is involved in modulation of tubulin assembly into microtubules (Bhattacharyya et al. 1985; Serrano et al. 1985; Sackett et al. 1989), and more recently, the C-terminal region has been shown to be involved in the binding of tubulin to the microtubule-associated protein Tau (Jimenez et al. 1999; Devred et al. 2004). Chemical modification of carboxyl groups of the protein eliminates the high-affinity calcium-binding site and reverses the induction of assembly by magnesium. Thus, when Ca^{2+} is added in excess of 1 mM, the assembly is inhibited (Mejillano and Himes 1991). This result and other evidence suggest that calcium binding occurs in this region and is important for the inhibition of tubulin polymerization in vitro (Weisenberg 1972; Serrano et al. 1986).

Both magnesium and calcium ions, at millimolar concentrations, diminish the fluorescence of DAPI, but previous studies have not determined whether they quench the fluorescence directly or displace the fluorescence probe from its binding site (Bonne et al. 1985). It was previously shown that Mg^{2+} displaces Mn^{2+} from the complex Mn–tubulin, but Ca^{2+} does not (Buttlaire et al. 1980; Ward and Timascheff 1988). These results suggest that Mg^{2+} and Ca^{2+} occupy different high-affinity binding sites, and hence the binding to these sites is not directly responsible for the quenching of DAPI bound to tubulin. Induction or inhibition of polymerization is produced in the millimolar range of these cations similar to the quenching effect on DAPI. However, little is known about the role of the low-affinity binding sites for Mg^{2+} and Ca^{2+} and their location.

In this study, the relative location of the DAPI-binding site on tubulin was determined through Förster Resonance Energy Transfer (FRET) using DAPI as a fluorescence donor and TNP–GTP and cobalt as acceptors (Fig. 1). Calculations on the molecular docking of DAPI to the tubulin heterodimer were performed and several candidate binding sites were found and discussed in the context of the energy transfer results.

Results

Dissociation constants of DAPI bound to tubulin, tubulin S, and to tubulin S–C-terminal peptides complex

The dissociation constants for complexes of DAPI with tubulin, tubulin S (in the GTP form), and the mixture of tubulin S plus C-terminal peptides (using a fixed tubulin S concentration) were determined by an anisotropy titration method, which circumvents potential artifacts inherent in intensity measurements (Jameson and Sawyer 1995; Jameson and Mocz 2005), based on the original observation of Weber (1952).

Specifically, the anisotropies of DAPI were followed at 20°C during the titration with tubulin and tubulin S, and the fraction of the probe bound to the proteins was calculated according to :

$$f_b = \frac{(r_{obs} - r_f)}{(r_b - r_{obs})Q + (r_{obs} - r_f)} \quad (1)$$

where r_{obs} is the observed anisotropy and r_f and r_b are the anisotropies of free and bound probe, respectively. Q is the relative quantum yield of the bound and free probe, and in this case, Q was determined to be 17.8.

The data in Figure 2A show that the increase in the anisotropy of DAPI produced by tubulin was higher than that of tubulin S, and in both cases, the anisotropy followed a hyperbolic saturation behavior. The same behavior was observed for the C-terminal peptides in the presence of tubulin S. The inset of Figure 2A shows the anisotropy increment of the complex DAPI–tubulin S when it was titrated with the C-terminal peptides. The experimental points shown in Figure 2A were fit to a hyperbolic equation and the r_b values were calculated for each curve. An r_f value of 0.125 was measured for the free probe in solution (which reflects the short lifetime of the free probe). The dependence on protein concentration of DAPI fraction bound to tubulin and tubulin S is shown in Figure 2B. The K_d values obtained from a 1:1 stoichiometry between ligand and protein (Bonne et al.1985) are shown in Table 1. In order to address the question of the possible influence of the fluorescent probe DAPI on the interaction between the C-terminal peptides and tubulin S, the N termini of the peptides were covalently labeled with FITC, since in both peptides, the N terminus residues are the only amino groups available, and the interaction of these peptides with tubulin S were studied in the absence of DAPI. Titration of C-terminal peptides, covalently bound to FITC with tubulin S, showed an anisotropy enhancement, which was not observed in the case of titration with tubulin. These results (data not shown) argue against the possibility that the binding of the C-terminal peptides to tubulin S is mediated by DAPI.

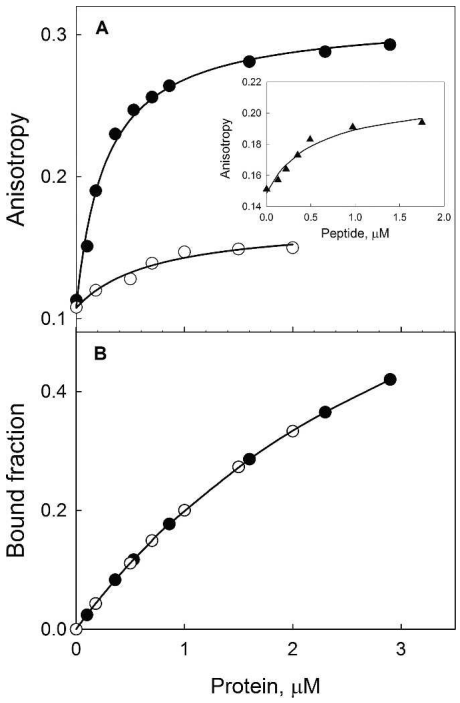

Figure 2. Changes in anisotropy (*A*) and DAPI fraction bound (*B*) during DAPI titration with tubulin, tubulin S, and the complex DAPI–tubulin S with the C-terminal peptides. Titration of 0.5 μM DAPI with tubulin (●) and tubulin S (○). The buffer used was 10 mM Tris-HCl (pH 7.5). The *inset* shows the titration of 0.5 μM DAPI plus 1.5 μM tubulin S with increasing concentrations of C-terminal peptides (▲). Excitation wavelength 350 nm; emission wavelength 455 nm; excitation and emission bandwidths were 2.5 and 12 nm, respectively.

Table 1. *Dissociation of the DAPI-protein complexes determined by fluorescence anisotropy*

Complex	K_D (μM)
DAPI-tubulin	5.2 ± 0.4 (3)[a]
DAPI-tubulin S	6.9 ± 2.3 (2)
DAPI-tubulin S plus C-terminal peptides	14.2 ± 4.7 (2)

All measurements were carried out at 20°C. Experimental conditions were as described in Figure 2.
[a] Number of experiments performed.

Fluorescence resonance energy transfer

In order to determine the location of the DAPI high-affinity binding site, and its relationship with the C-terminal region of tubulin, FRET experiments were designed to determine the distance between DAPI and the Co(II) cation bound to the nonexchangeable site, as well as TNP–GTP bound to the exchangeable site. The concentration of DAPI was 2 μM (pH 7.0) with 0.1 mM GTP in the absence of cations. Due to the absence of free magnesium, the experiments had to be carried out on freshly prepared protein during the period of time in which the protein was stable. Figure 3 shows the fluorescence emission spectrum of the DAPI–tubulin complex, with a maximum at 452 nm, the absorption spectra of Co(II)–tubulin complex with a shoulder of absorbance at 420 nm, and the TNP–GTP–tubulin complex with two absorbance maxima at 408 and 470 nm. From the overlap of the DAPI emission and Co(II) absorption spectra, the spectral overlap integral, J(λ), was calculated by numerical integration over 2-nm intervals and was found to be 2.54×10^{-16} M^{-1} cm^3. From the overlap of the DAPI emission and the TNP–

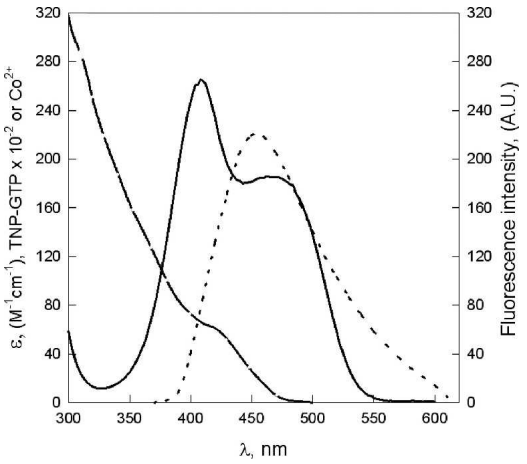

Figure 3. Overlap of the absorption spectra of tubulin–cobalt and tubulin TNP–GTP complexes with the fluorescence emission spectrum of DAPI–tubulin complex. The spectra were obtained in 10 mM triethanolamine, 0.1 mM GTP (pH 7.0), at 25°C. The absorption spectrum of 0.16 mM tubulin–cobalt complex containing 0.8 mol/mol of cobalt (segmented line) was recorded using an identical concentration of tubulin–magnesium as a control. The absorption spectrum of one mole of TNP–GTP, bound at the E-nucleotide binding site, was recorded (solid line). The fluorescence emission spectrum of 2 μM DAPI with 7.9 μM tubulin (dashed line) was recorded using an excitation wavelength of 350 nm and excitation and emission bandwidth of 2.5 nm.

GTP absorption spectra, J(λ) was calculated to be 7.29×10^{-14} M^{-1} cm^3. The quantum yield of DAPI–tubulin complex with magnesium as a control was 0.63. The measured quantum yield of the DAPI–tubulin complex in the presence of cobalt as a fluorescent acceptor was 0.50 and in the presence of TNP–GTP it was 0.31. The observed molar fractional occupancy, determined as indicated in the Materials and Methods, was 0.80 ± 0.06 and 0.97 ± 0.16 for cobalt and TNP–GTP, respectively. According to Equation 3, the efficiency of the energy transfer was calculated to be 0.26 for the DAPI–Co energy transfer and 0.51 for the DAPI–TNP–GTP energy transfer. Assuming a value of 2/3 for κ^2 in both transfers, R_0 was calculated from Equation 4 to be 17 and 43 Å, respectively. From these values and the efficiencies of energy transfer, a value of 20 ± 2 Å (where these numbers represent the average of two independent determinations) was estimated for the distance between the DAPI-binding site and the cobalt high-affinity binding site. The calculated distance between DAPI and the TNP–GTP located at the exchangeable site in β-tubulin, was 43 ± 2 Å (three independent determinations). However, the assumption of 2/3 for κ^2 in this system must be examined as discussed below.

DAPI–tubulin molecular docking

The results of the molecular docking calculations are summarized in Table 2. Initially, many potential DAPI-binding sites were identified with widely differing affinities. Eight sites with affinities higher than the binding affinities determined using fluorescence anisotropy were found and are shown in Figure 4. The theoretical ΔΔG values for these eight sites, found through the molecular docking calculations, are shown in Table 2. The distances in Table 2 were measured from carbon 2 of the indole ring of DAPI to the 3′-carbon on the ribose ring of TNP–GTP (see Fig. 1) and also to the magnesium ion, in the non-exchangeable nucleotide-binding site, replaced by cobalt in the experimental system. Figure 5 shows the three-dimensional structure of the DAPI-binding site on tubulin that corresponds to site number II in Table 2.

Discussion

The dissociation constants of the binary complexes DAPI–tubulin and DAPI–tubulin S were found to be 5.2 ± 0.4 and 6.9 ± 2.3 μM, respectively, as determined by fluorescence anisotropy at 20°C. It is apparent from these values that the binding of DAPI to tubulin and to tubulin S does not depend significantly on the presence of the C-terminal region. Hence, the decrease in the fluorescence intensity of DAPI bound to tubulin, induced by the removal of this region, could be due to an increase in the accessibility of the probe to solvent, with the subsequent reduction in the quantum yield of the fluorophore. The initial possibility that the binding of the C-terminal peptides to tubulin S was mediated by DAPI, as suggested by Bonne et al. (1985) who proposed that the binding site of DAPI was located at the C-terminal region, was subsequently considered unlikely because these peptides covalently labeled with the fluorescent probe FITC were able to bind to tubulin S in the absence of DAPI (Ortiz et al. 1993).

Table 2. *Molecular docking binding parameters and distances to Co^{2+} and TNP–GTP of DAPI bound to tubulin heterodimer*

		Distances (Å)	
Site number	ΔΔG kcal/mol	DAPI-TNP-GTP	DAPI -Co^{2+}
I	−18.16	56	27
II	−17.78	30	21
III	−17.46	40	25
IV	−16.71	37	30
V	−16.66	37	20
VI	−16.13	54	31
VII	−15.87	37	16
VIII	−15.57	39	14

The binding sites and their free energy of binding were determined with the computer program Autodock v3.05. Distances were determined with the distance routine of the computer program Swiss-PdB Viewer v. 3.7 b2.

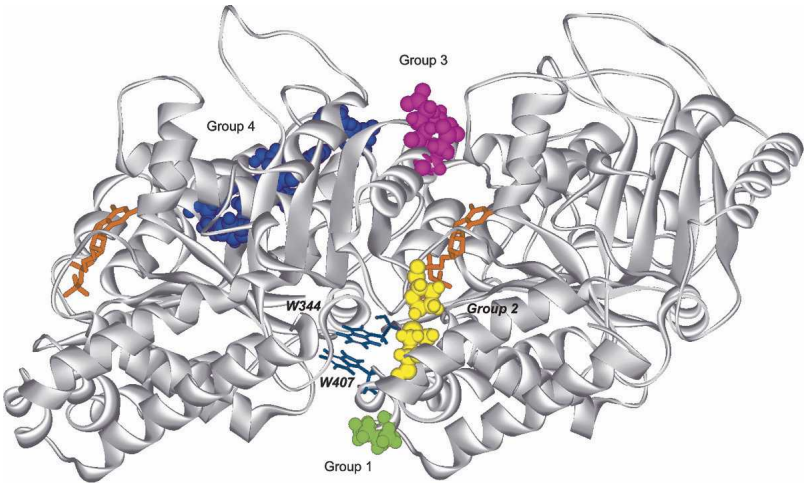

Figure 4. DAPI surrounding amino acid group selected on the basis of the FRET results shown in the ribbon three-dimensional structure of tubulin heterodimer. The three-dimensional structure of tubulin heterodimer was drawn with the computer program package DS Modelling 1.1. The nucleotides are shown in orange at the E-site in β-tubulin (GDP) and at the N-site in α-tubulin (GTP). The amino acids indicated were selected as described in the text. The selected groups of amino acids are indicated by different colors. Group 1 (green); Group 2 (yellow); Group 3 (fuchsia); Group 4 (blue). The tryptophan residues closest to Groups 1 and 2 are also indicated.

In order to know the location and the structural characteristic of the DAPI high-affinity binding site, FRET and computational docking calculations were carried out. The location of the high-affinity DAPI site on tubulin was determined by triangulation of the distances of this site to the cobalt-binding site at the nucleotide N-site and to the sugar moiety of the nucleotide bound at the E-site, as described below.

The distance between the DAPI-binding site and the magnesium (replaced by cobalt) high-affinity binding site was 20 ± 2 Å, and the distance between DAPI and the nucleotide fluorescence probe TNP–GTP located at the E-site was initially taken as 43 ± 2 Å. It has been suggested that the cation high-affinity binding site is located on the nonexchangeable nucleotide-binding site (N-site) in α-tubulin (Menendez et al. 1998). The N-site in the microtubule is buried at the intradimer interface between both tubulin monomers (Nogales et al. 1999; Huilin et al. 2002). Ward and Timasheff (1988), using FRET, determined that the distance between Co^{2+}, located at the high-affinity binding site, and the drugs colchicine and allocolchicine were larger than 17 and 24 Å, respectively. The colchicine-binding site is located close to the αβ intradimer interface where the main part of this site is located on the β-tubulin. Colchicine forms hydrogen bonds with Asn 101α Cys 241β, and it is close to Val 257β and Val 351β in αβ-tubulin complexed with colchicine and a stathmin-like domain (PDB 1SAO) (Ravelli et al. 2004).

Although the three-dimensional structure of tubulin (PDB; TUB1JFF) was determined at low resolution, the average distance of 17 Å between the colchicine and taxol-binding sites measured by Han et al. (1998), is in agreement with that determined from the structure. Also from the structure, it is possible to determine a distance of 14 Å between the magnesium located at the N-site and the SH group of the Cys 354β located close to the colchicine-binding site, which agrees within experimental error with the distance determined by Ward and Timasheff (1988). At the first sight, the similarity in the distance from colchicine and DAPI to the cobalt high-affinity site could indicate that they share the same region in the heterodimer; however, the results of Bonne et al. (1985) led us to discard this idea, because DAPI binds with the same apparent association constant to tubulin in the presence of colchicine, indicating that both sites are independent.

In order to define the region wherein the DAPI-binding site could reside, a spherical subset of the amino acid residues was constructed from the three-dimensional structure of tubulin (1TUB.pdb), using as a center magnesium located at the N-site. The selected atoms were those that were between the spheres with radii of 21 and 17 Å, which correspond to an average distance of 19 ± 2 Å. The same criteria were used for the distance between DAPI and TNP–GTP located at the E-site on β-tubulin. A point located at the C′3 of the sugar ring of the nucleotide, at the E-site, was used as a center. This point is 4 Å from the center of the fluorescence moiety of the TNP–GTP in the same plane of the sugar ring. The selected atoms were those located in the space between the spheres with an inner and outer radius of

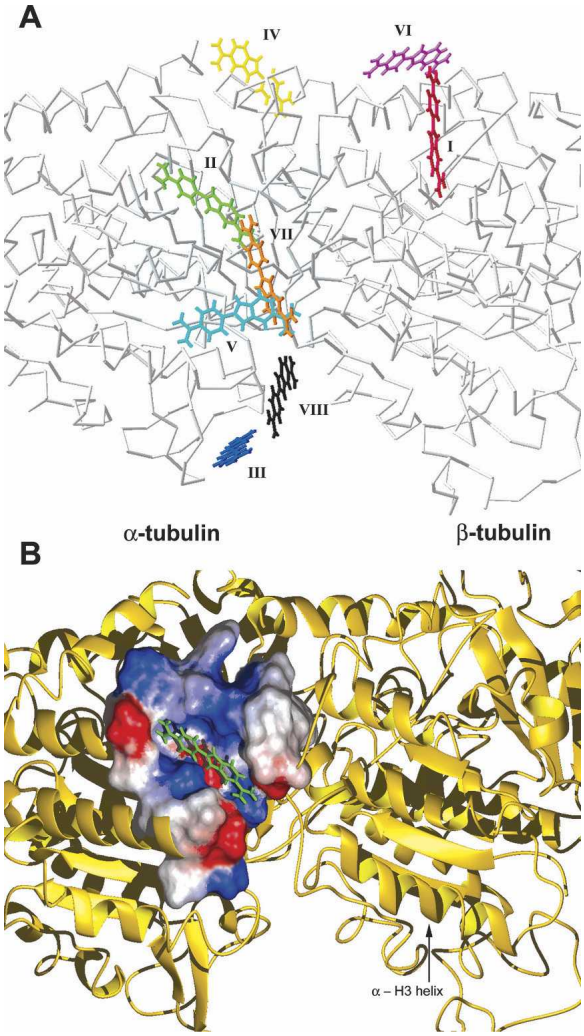

Figure 5. Computer molecular models of DAPI-binding sites on tubulin heterodimer. The models and location of DAPI-binding sites in the three-dimensional structure of tubulin heterodimer were built by computer molecular docking with the program Autodock v. 3.0.5 as explained in the Material and Methods. (*A*) The three-dimensional structure of tubulin heterodimer and DAPI were drawn (backbone) with the program Viewer Lite 5.0, Accelrys Inc. The binding sites with DAPI bound are indicated by different colors and with Roman numerals. Site I (red); site II (green); site III (dark blue); site IV (yellow); site V (light blue); site VI (fuchsia); site VII (brown); site VIII (black). (*B*) Part of the three-dimensional structure of tubulin and the binding site II with DAPI (green) were drawn (ribbons) with the program Mol Mol using surface potentials. This site is shown as van der Waals surface, colored according to the electrostatic potentials. As a reference of the molecule position, the helix H3 of α-tubulin is indicated.

37 and 41 Å, respectively, which corresponds to an average distance of 39 ± 2 Å. This distance is the result of the experimental 43 ± 2 Å minus the 4 Å, as previously explained. Four regions of amino acids that belong to both spheres were selected as belonging to the DAPI-binding site. Most of the amino acids selected were around the contact zone of the α- and β-tubulin monomers, and this approach is illustrated in Figure 4. They were mostly located at the interface between both subunits and they were divided into four groups of amino acid residues, as follows: (1) G410α and V409α; (2) M398α and P346β; (3) S322β, E325β, and E328β; (4) Y36β, D41β, S40β, E27β, F20β, H28β, and I24β (Table 3).

As mentioned earlier, the experimentally derived distance for TNP–GTP to DAPI, 43 Å, was determined using a κ^2 value of 2/3, which assumes dynamic averaging of the donor and acceptor dipoles. In fact, the anisotropies observed for both DAPI and TNP–GTP bound to tubulin were high, 0.372 and 0.327, respectively. One may then consider the FRET data from another point of view. Namely, one can calculate what values of κ^2 would be required for the donor/acceptor pair to give the distances determined from the MD calculations. If we consider the two putative-binding sites, which correspond to the 20–21 Å distances for the DAPI–Cobalt pairs (since the uncertainty in this value is likely to be low given the symmetry of the acceptor dipole), we must choose between the TNP–GTP distances of 30 and 37 Å. In order to reduce the R_0 value sufficiently to yield these distances from the FRET data, the κ^2 values would have to be 0.07 and 0.30, respectively. Given the observed ratios of the anisotropies for the donor and acceptor probes bound relative to their limiting values (0.93 and 1.00 for DAPI and TNP–GTP, respectively) one can consult

Table 3. *Properties of the selected regions of αβ-tubulin heterodimer determined from the spherical subsets of amino acids constructed with the FRET distances*

Group[a]	Correspondence[b]	Residues	Location[c]	Nearest Trp[d]
1	Docking site II	Val409 α Gly410 α	LN-Out	Trp407 α (8.1 Å)
2	Docking site IV	Met398 α Pro346 β	Out	Trp344 β (8.0 Å)
3	No	Phe20 β Ile24 β Glu27 β His28 β Tyr36 β Ser40 β Asp41 β	In	No
4	Docking site III	Ser322 β Glu325 β Glu328 β	L2-In	No

[a] The groups correspond to that shown in Figure 4.
[b] The location of the groups were compared in the three dimensional structure of tubulin with that of the docking sites shown in Figure 5A.
[c] The location of the groups are (In) inside, (Out) outside, (LN) lateral contact through the nucleotide side, (L2) lateral contact with the second domain, as defined by Nogales et al. (1998b).
[d] The distance between the CE3-Trp407 α and CH2-Trp344 β to the centroid of the amino acid lateral chains of the group was measured with the computer program DS Modelling 1.1 from Accelrys.

the plots calculated by Dale et al. (1979) to see the theoretical limits for κ^2. In fact, this range turns out to be ~0.02–3.7. Hence, both the 30 and 37 Å sites (sites II and V in Table 2) fall in this range, and one cannot distinguish—on the basis of the TNP–GTP FRET data—between these two binding sites.

One may then ask whether there are any other criteria that can be used to choose between these two potential DAPI sites. For example, one may consider the experimental observation of energy transfer between the intrinsic tryptophan emission and DAPI that was reported by Bonne et al. (1985). We also measured the excitation spectra of DAPI free and bound to tubulin and noted a significant increase in the region of the protein absorption (270–290 nm), which can be attributed to tryptophan to DAPI energy transfer (data not shown). However, we note (Table 3) that site II is located within a distance of 8.1 Å from Trp 407 of α-tubulin and that site IV has the tryptophan 344 β residue in relatively close proximity (8.0 Å), and given the inherent uncertainty in the FRET efficiencies of these tryptophan residues to DAPI (since differences in their respective emission spectra may compensate for the slight distance difference), one cannot rigorously use tryptophan data to choose between the sites.

Finally, other criteria that can be used to localize the DAPI-binding site include the following observations: (1) the last amino acid residues of the C-terminal region of β-tubulin, which are removed by subtilisin, should be able to influence the solvent accessibility of this site (Ortiz et al. 1993); (2) the site should be in a pocket with negative charges and a hydrophobic region, where DAPI, with its two positive charges, separated by around 12.5 Å, could fit (Vlieghe et al. 1999); and (3) the binding site should be located in a region accessible to the solvent in the tubulin heterodimer or in the microtubule, because when DAPI binds to each of these forms, both fluorescence-emission maxima are at 446 nm (Ortiz et al. 1993).

The regions where the first and the second group of amino acids (V405α, V409α, G410α, and P348β) are located in the external face of the microtubule meet all of the conditions mentioned above. On the other hand, the site close to the third group (E328β and L331β) is involved in the longitudinal interaction of protofilaments in the microtubule interfering with the access of DAPI (Nogales et al. 1999; Huilin et al. 2002). Finally, the molecular docking of DAPI on tubulin heterodimer showed that the calculated binding constants are higher than that determined experimentally. A reasonable explanation is that the crystal structure of DAPI used for the docking calculations assumed net positive charges at the N-terminal groups, which increases the value of ΔΔG for the dissociation of DAPI from tubulin. Of the eight probable binding sites for DAPI (Table 2), site II, which is located close to the interface of both tubulin monomers, is the most reasonable location, because the experimental distances and the other properties discussed above are consistent with this location. This site, indicated in Figure 5, shares two negative-charged zones separated by a positive and noncharged zone where the rings of DAPI fit correctly.

Materials and methods

Reagents

GTP (type III), subtilisin-agarose, TEA, DAPI, Tris, glycerol, fluorescamine, FITC (isomer I), EGTA, sodium phosphate, maleic acid, MES, guanidine hydrochloride, Sephadex G-25, and DEAE-Sephadex A-50 were purchased from Sigma Chemical Co. Sephacryl S-300 HR was from Amersham Pharmacia Biotech. Salts and solvents were analytical grade obtained from Merck. Bio-Gel P-60 was from Bio-Rad Laboratories Inc. Nanopure grade water was used throughout.

Chicken brain tubulin purification

Brains were dissected from freshly slaughtered chickens (kindly provided by Industrial Ochagavia Ltda.), kept on ice, and used within 2 h. Tubulin was purified by the method of Weisenberg et al. (1968) and Weisenberg and Timasheff (1970), as modified by Lee et al. (1973) and Monasterio (1987). The stock protein with 1 M sucrose was stored at –80°C. In order to eliminate the aggregates from the stock protein, the experimental samples were filtrated through a Sephacryl S-300 column (0.5×25 cm) at a flux rate of 0.5 mL/min, at 4°C equilibrated with the experimental buffer. Only the fractions corresponding to the heterodimer were used.

Protein determination

Protein concentrations were determined by measuring the absorbance at 275 nm of samples diluted 10-fold in 6 M guanidinium chloride, using an absorptivity value of 1.03 L g^{-1} cm^{-1} (Na and Timasheff 1981). C-terminal peptide concentrations were determined with fluorescamine as described by Bohlen et al. (1973); fluorescence was measured at 475 nm using an excitation wavelength of 390 nm.

Proteolytic digestion

The digestion of tubulin was carried out as described by Ortiz et al. (1993). To obtain tubulin S, tubulin (2 mg/mL) was incubated with subtilisin-agarose (0.2 U) in 10 mM TEA (pH 7.0), 0.1 mM GTP, 0.2 mM $CaCl_2$, and 25% glycerol, at 30°C for 1 h with occasional stirring. TEA was used because tubulin S aggregation was the lowest with respect to other buffers assayed, yielding, under these conditions, a better yield of tubulin S. Tubulin digestion products, α- and β-tubulin C-terminal peptides and tubulin S, were isolated from subtilisin-agarose by centrifugation at 1000*g*. The supernatant was chromatographed at 4°C in a 0.8×25-cm Bio-Gel P-60 column, previously equilibrated with 10 mM Tris-HCl (pH 7.0), and

the fractions corresponding to tubulin S were collected. To obtain tubulin C-terminal peptides, the digestion was performed as above, but the buffer was replaced by 0.1 M MES, 15 mM $MgCl_2$, 0.1 mM GTP (pH 6.4), incubated 3 h at 10°C with occasional stirring, and centrifuged to separate the subtilisin-agarose. Tubulin S aggregates in buffer MES, which facilitates the purification of peptides. The supernatant was mixed with 1 mL of DE-52 equilibrated in 10 mM phosphate buffer (pH 7.0) for 5 min, and centrifuged. The supernatant was discarded, and the resin was washed two times with the equilibration buffer plus 0.2 M NaCl. Tubulin C-terminal peptides were eluted with the equilibration buffer plus 0.5 M NaCl. The peptides were concentrated through dialysis against sucrose and then dialyzed against the experimental buffer. The purity of the different digestion products of tubulin were analyzed by electrophoresis in SDS–urea polyacrylamide gels as described by Ortiz et al. (1993). Analysis by reverse-phase HPLC in a C-18 column shows that the digested peptide's composition was not affected by the buffers MES or TEA used in the controlled digestion.

Divalent cation determination

The content of divalent cations was determined by atomic absorption spectroscopy in a Perkin-Elmer Model 303 spectrometer as reported by Monasterio and Timasheff (1987).

Preparation of TNP–GTP–tubulin complex

The exchange of the nucleotide at the E-site in tubulin was performed as indicated by Han et al. (1998). The TNP–GTP-binding stoichiometry was measured in 100 mM PIPES, 1 mM $MgSO_4$ and 2 mM EGTA (pH 6.9). The samples containing the complex TNP–GTP-tubulin, plus 50 μM TNP–GTP were filtrated by centrifuging a MICROCON 30 system at 5585*g* in a COSTAR minicentrifuge at room temperature. The free concentration of TNP–GTP was determined in the filtrate at 408 nm using a molar absorption coefficient of 2.3×10^4 M^{-1} cm^{-1}. Due to the presence of TNP–GTP, the concentration of tubulin (MW 110,000) was determined by the Bradford method using the Bio-Rad kit of reagents. Bound TNP–GTP was calculated as the difference between the total and the free concentration of TNP–GTP, value that, divided by the protein concentration, gives the stoichiometry.

Absorption and fluorescence spectroscopy

Absorption spectra were obtained on a Hewlett-Packard 8452A diode array spectrophotometer. Steady-state fluorescence measurements were made on a Perkin-Elmer LS50 luminescence spectrometer equipped with the FLDM program and film polarizers or on an ISS Greg 200 spectrofluorometer (ISS, Inc.) equipped with calcite prism polarizers. Fluorescence quantum yields were measured relative to quinine sulfate in 0.1 N sulfuric acid at 20°C, using $\Phi = 0.55$ (Melhuish 1961).

Fluorescence resonance energy transfer

The distances between DAPI and cobalt and DAPI and TNP–GTP, bound to tubulin were determined by fluorescence energy transfer (Förster 1948). The efficiency for this process from a fluorescent donor to an acceptor is given by:

$$E = \frac{R_0^6}{R^6 + R_0^6} \tag{2}$$

where R is the distance between donor and acceptor and R_0 is the distance at which the transfer efficiency is 0.5. E can be experimentally determined by measuring the quantum yield in the presence (F_{da}) and in the absence (F_d) of the energy acceptor. Since tubulin has one high-affinity site for DAPI (Bonne et al. 1985), but only binds a molar fraction (f_a) of cobalt, this effect must be considered in the energy transfer efficiency calculation (Cheung 1991):

$$E = 1 - \frac{F_{da} - F_d(1 - f_a)}{F_d f_a} \tag{3}$$

The critical distance, R_0, can be calculated according to:

$$R_0 = 9.78 \times 10^3 (\kappa^2 F_d \, J(\lambda) \, \eta^{-4})^{1/6} \quad [\text{Å}] \tag{4}$$

where η is the refractive index of the medium, κ^2, the orientation factor that depends on the angles between the transition moments of the donor and acceptor, and J(λ), the spectral overlap integral. The latter is given by:

$$J(\lambda) = \int_0^\infty F(\lambda)\varepsilon(\lambda)\lambda^4 d\lambda \quad [\text{M}^{-1}\text{cm}^3] \tag{5}$$

where F(λ) is the fluorescence spectrum of the donor normalized to unity, and ε(λ) is the absorption spectrum of the acceptor. R_0 was calculated using a value of 1.368 for the refractive index of the medium, measured in a Galileo 22701 refractometer, and a value of 2/3 was used for κ^2. This value corresponds to a rapid reorientation between donor and acceptor transition electronic moments. Cobalt has a spherical symmetry with triply degenerate transitions polarized along mutually perpendicular orientations, which approximates an isotropic oscillator; this symmetry reduces the uncertainty in $\langle\kappa^2\rangle$ (Dale et al. 1979).

Molecular modeling of DAPI docking

The automated docking of the flexible DAPI molecule on the fixed tubulin heterodimer was performed. Data for tubulin structure were obtained from the files 1JFF.pdb and 1TUB.pdb. The coordinates for DAPI structure were obtained from the file 1D3O.pdb.

Due to the low resolution for the tubulin structure found in the file 1TUB.pdb (3.7 Å) and the problems found when the initial energy for this structure was evaluated with the computer program AUTODOCK 3.05 (academic version), a new model for the structure of tubulin was built using the file 1JFF.pdb (resolution 3.5 Å), which does not present problems with the initial energy calculation. The structure of α-tubulin in the file 1JFF was supplemented with the structure of the 26 amino acids, from residues 33 to 59, using the coordinates given in the file 1TUB.pdb for the structure of these peptide residues. To fit the structure of the 26 amino acid peptide in α-tubulin, the computer program MODELLER v6.2 was used.

The hydrogen atoms and partial charges at pH 7.0 were assigned to the tubulin model with the computer program DISCOVER using the force field AMBER from the software package ACCELRYS INSIGHTII version 98 (we thank Dr. Gerald Zapata [Universidad de Chile], who allowed us access to these programs). The partial charges of DAPI were assigned considering the charge values of the amino acids tryptophan, arginine, and phenylalanine available in the force field AMBER. In order to assign the aromatic carbons, the computer program AUTOTORS that belongs to the AUTODOCK software package was used. Rotation of the intramolecular bonds of DAPI was not allowed.

Solvent effects were added to the model of tubulin with the computer program AUTODOCK v3.05. To generate the working grids, a basic grid of $126\times126\times126$ dots with 0.375 Å of distance between them, was used. To calculate the number of grids necessary to cover the surface of the tubulin model, a script was built using PERL. In the search of the DAPI-binding sites, the surface of the protein was completely covered with grids, each one overlapping its neighbor by 10 Å. With these grids, the binding sites of DAPI were calculated using the Lamarckian algorithm that is configured in the computer program AUTODOCK v3.05. The number of runs per grid was 20. The binding sites with the higher ΔG values were selected and inspected visually with the computer program Swiss-PdB Viewer v3.7 b2.

Acknowledgments

We thank Andrea Garcés for assistance with the computer drawing of the figures. This work was supported by Grants 7050057, 1010848, and 1050677 from FONDECYT (Chile).

References

Barcellona, M.L. and Gratton, E. 1990. The fluorescence properties of a DNA probe: 4′-6-Diamidino-2-phenylindole (DAPI). *Eur. Biophys. J.* **17:** 315–323.

Bhattacharyya, B., Sackett, D. L., and Wolff, J. 1985. Tubulin hybrid dimers, and tubulin S. *J. Biol. Chem.* **260:** 10208–10216.

Bhattacharyya, A., Bhattacharyya, B., and Roy, S. 1993. A study of colchicine tubulin complex by donor quenching of fluorescence energy transfer. *Eur. J. Biochem.* **216:** 757–761.

Bhattacharyya, A. Bhattacharyya, B., and Roy, S. 1994. Magnesium-induced structural changes in tubulin. *J. Biol. Chem.* **269:** 28655–28661.

Bhattacharyya, A., Bhattacharyya, B., and Roy, S. 1996. Fluorescence energy transfer measurement of distances between ligand binding sites of tubulin and its implication for protein-protein interaction. *Protein. Sci.* **5:** 2029–2036.

Bohlen, P., Stein, S., Dairman, W., and Udenfriend, S. 1973. Fluorimetric assay of protein in the nanogram range. *Arch. Biochem. Biophys.* **155:** 213–220.

Bonne, D., Heusele, C., Simon, C., and Pantaloni, D. 1985. 4′,6-Diamidino-2-phenylindole, a fluorescent probe for tubulin and microtubules. *J. Biol. Chem.* **260:** 2819–2825.

Bryan, J. and Wilson, L. 1971. Are cytoplasmic microtubules heteropolymers? *Proc. Natl. Acad. Sci.* **68:** 1762–1766.

Buttlaire, D.H., Czuba, B.A., Stevens, T.H., Lee, Y.C., and Himes, R.H. 1980. Manganous ion binding to tubulin. *J. Biol. Chem.* **255:** 2164–2168.

Cheung, H.C. 1991. Resonance energy transfer. In *Topics in fluorescence spectroscopy* (ed. J.R. Lakowicz), Vol. 2, pp. 127–176, Plenum, New York.

Dale, R.E., Eisenger, J., and Blumberg, W.E., 1979. The orientation freedom of molecular probes. *Biophys. J.* **26:** 161–193.

Devred, F., Barbier, P., Douillard, S., Monasterio, O., Andreu, J.M., and Peyrot, 2004. Tau induces ring and microtubule formation from αβ-tubulin dimers under nonassembly conditions. *Biochemistry* **43:** 10520–10531.

Förster, T. 1948. Intermolecular energy migration and fluorescence. *Ann. Phys. (Leipzig)* **2:** 55–75. (Translated by R.S. Knox.)

Hajduk, S.L. 1976. Demonstration of kinetoplast DNA in dyskinetoplastic strains of Trypanosoma equiperdum. *Science* **191:** 858–859.

Han, Y., Malak, H., Chaudhary, A.G., Chordia, M.D., Kingston, D.G., and Bane, S. 1998. Distances between placlitaxel, colchicine and exchangeable GTP binding sites on tubulin. *Biochemistry* **37:** 6636–6644.

Huilin, L., DeRosier, D.J., Nicholson, W.V., Nogales, E., and Downing, K.H. 2002. Microtubule structure at 8 Å resolution. *Structure* **10:** 1317–1328.

Grossgebauer, K., Kegel, M., and Dann, O. 1976. New fluorescent microscopical technique in diagnostic microbiology. *Dtsh. Med. Wochenschr.* **101:** 1098–1099.

Jameson, D.M. and Mocz, G. 2005. Fluorescence polarization/anisotropy approaches to study protein–ligand interactions: Effects of errors and uncertainties. *Mol. Biol.* **305:** 301–322.

Jameson D.M. and Sawyer, W.H. 1995. Fluorescence anisotropy applied to biomolecular interactions. *Methods Enzymol.* **246:** 283–300.

Jimenez, M.A., Evangelio, J.A., Aranda, C., Lopez-Brauet, A., Andreu, D., Rico, M., Lagos, M., Andreu, J.M., and Monasterio, O. 1999. Helicity of α(404) and β(394–445) tubulin C-terminal recombinant peptides. *Protein Sci.* **8:** 788–799.

Kung, C.E. and Reed, J.K. 1989. Fluorescent molecular rotors: A new class of probes for tubulin structure and assembly. *Biochemistry* **28:** 6678–6686.

Lee, J.C., Frigon, R.P., and Timasheff, S.N. 1973. The chemical characterization of calf brain microtubule protein subunits. *J. Biol. Chem.* **248:** 7253–7262.

Mazzini, A., Cavatorta, P., Iori, M., Favilla, R., and Sartor, G. 1992. The binding of 4′,6-diamidino-2-phenylindole to bovine serum albumin. *Biophys. Chem.* **42:** 101–109.

Mejillano, M.R. and Himes, R.H. 1991. Assembly properties of tubulin after carboxyl group modification. *J. Biol. Chem.* **266:** 657–664.

Melhuish, W.H. 1961. Quantum efficiencies of fluorescence of organic substances: Effect of solvent and concentration of the fluorescent solutes. *J. Phys. Chem.* **65:** 228–235.

Melki, R., Kerjan, P., Waller, J.P., Carlier, M.F., and Pantaloni, D. 1991. Interaction of microtubule associated proteins with microtubules: Yeast lysyl- and valyl-tRNA synthetases and τ 218–235 synthetic peptide as model systems. *Biochemistry* **30:** 11536–11545.

Menendez, M., Rivas, G., Diaz, J.F., and Andreu, J.M. 1998. Control of the structural stability of the tubulin dimer by one high affinity bound magnesium ion at nucleotide N-site. *J. Biol. Chem.* **273:** 167–176.

Monasterio, O. 1987. ^{19}F Nuclear magnetic resonance measurement of the distance between the E-Site GTP and the high-affinity Mg^{2+} in tubulin. *Biochemistry* **26:** 6100–6106.

Monasterio, O. and Timasheff, S.N. 1987. Inhibition of tubulin self-assembly and tubulin colchicine GTPase activity by guanosine-5′-(γ-fluorotriphosphate). *Biochemistry* **26:** 6091–6099.

Monasterio, O., Andreu, J.M., and Lagos, R. 1995. Tubulin structure and function. *Comments Mol. Cell. Biophys.* **8:** 273–306.

Na, G.C. and Timasheff, S.N. 1981. Interaction of calf brain tubulin with glycerol. *J. Mol. Biol.* **151:** 165–178.

Nogales, E., Wolf, S.G., and Dowing, K.H. 1998a. Structure of the αβ tubulin dimer by electron crystalography. *Nature* **391:** 199–203.

Nogales, E., Downing, K.H., Amos, L.A., and Löwe, J. 1998b. Tubulin and FtsZ form a distinct family of GTPases. *Nat. Struct. Biol.* **5:** 451–458.

Nogales, E., Whittaker, M., Milligan, R.A., and Downing, K. 1999. High-resolution model of the microtubule. *Cell* **96:** 79–88.

Ortiz, M., Lagos, R., and Monasterio, O. 1993. Interaction between the C-terminal peptides of tubulin and tubulin S detected with the fluorescent probe 4′,6-diamidino-2-phenylindole. *Arch. Biochem. Biophys.* **303:** 159–164.

Prasad, A.R.S., Luduena, R.F., and Horowitz, P.M. 1986. Detection of energy transfer between tryptophan residues in the tubulin molecule and bound bis(8-anilinonaphtalene-1-sulfonate), an inhibitor of microtubule assembly, that binds to a flexible region on tubulin. *Biochemistry* **25:** 3536–3540.

Ravelli, R.B., Gigant, B., Curmi, P.A., Jourdain, I., Lachkar, S., Sobel, A., and Knossow, M. 2004. Insight into tubulin regulation from a complex with colchicine and a stathmin-like domain. *Nature* **428:** 198–202.

Russell, W.C., Newman, C., and Williamson, D.H. 1975. A simple cytochemical technique for demonstration of DNA in cells infected with mycoplasmas and viruses. *Nature* **253:** 461–462.

Sackett, D.L., Zimmerman, D.A., and Wolff, J. 1989. Tubulin dimer dissociation and proteolytic accessibility. *Biochemistry* **28:** 2662–2667.

Serrano, L., Montejo de Garcini, E., Hernández, M., and Avila, J. 1985. Localization of the tubulin binding site for τ protein. *Eur. J. Biochem.* **153:** 595–600.

Serrano, L., Valencia, A., Caballero, R., and Avila, J. 1986. Localization of the high affinity calcium-binding site on tubulin molecule. *J. Biol. Chem.* **261:** 7076–7081.

Soto, C., Rodriguez, P., and Monasterio, O. 1996. Calcium and gadolinium ions stimulate the GTPase activity of purified chicken brain tubulin through a conformational change. *Biochemistry* **35:** 6337–6344.

Vlieghe, D., Sponer, J., and Meervelt, L.V. 1999. Crystal structure of d(GGCCAATTGG) complexed with DAPI reveals novel binding mode. *Biochemistry* **38:** 16443–16451.

Ward, L. and Timasheff, S.N. 1988. Energy-transfer studies of the distance between the high-affinity binding site and the colchicine and 8-anilino-1-naphthalesulfonic acid binding sites on calf brain tubulin. *Biochemistry* **27:** 1508–1514.

Ward, L.D., Seckler, R., and Timasheff, S.N. 1994. Energy-transfer studies of the distances between the colchicine, ruthenium red and bis ANS binding sites on calf brain tubulin. *Biochemistry* **33:** 11900–11908.

Weber, G. 1952. Polarization of the fluorescence of macromolecules. 1. Theory and experimental method. *Biochem. J.* **51:** 145–155.

Weisenberg, R.C. 1972. Microtubule formation in vitro in solutions containing low calcium concentrations. *Science* **177:** 1104–1105.

Weisenberg, R.C. and Timasheff, S.N. 1970. Aggregation of microtubule subunit protein. Effects of divalent cations, colchicine and vinblastine. *Biochemistry* **9:** 4110–4116.

Weisenberg, R.C., Borisy, G.G., and Taylor, E.W. 1968. The colchicine-binding protein of mammalian brain and its relation to microtubules. *Biochemistry* **7:** 4466–4479.